

Corrosivity of Fluids as a Function of the Distillate Cut: Application of an Advanced Distillation Curve Method

Lisa Starkey Ott and Thomas J. Bruno*

Physical and Chemical Properties Division, National Institute of Standards and Technology (NIST),
Boulder, Colorado 80305

Received April 20, 2007. Revised Manuscript Received June 15, 2007

Recently, we reported a method and apparatus for the advanced measurement of distillation curves. The new method allows for increased precision in the measurement of distillation curves as well as a composition-explicit channel of data. Herein, we report a further extension of this method, one which provides the capability to assess corrosivity and quantitate corrosive impurities (such as acidic sulfur species commonly found in fuel feedstocks) as a function of the distillate fraction. To demonstrate the new metrology, we examined mixtures of *n*-decane and *n*-tetradecane with dissolved H₂S. At each of 11 predetermined distillate volume fractions, the corrosivity was measured with the copper strip corrosion test (CSCT) and the sulfur concentration was measured by gas chromatography with sulfur chemiluminescence detection. Significantly, we were able to quantitatively correlate the distillation temperature of the fluid with both the sulfur concentration and the results of a CSCT for samples that had initial sulfur concentrations that differed 15-fold.

Introduction

Advanced Distillation Curve Method. One of the most important and informative properties that is measured for fluid mixtures is the distillation (or boiling) curve.^{1–3} The distillation curve is simply a graphical depiction of the boiling temperature of a fluid mixture plotted against the volume fraction distilled. One most often thinks of distillation curves in the context of petrochemicals and petroleum refining, but such curves are of great value in assessing the properties of any complex fluid mixture.

The standard test method, (ASTM) D-86,⁴ provides the usual approach to the measurement of the distillation curve. The data obtained with ASTM D-86 are the initial boiling point (IBP), the temperature at predetermined distillate volume fractions, as well as the final boiling point (FBP). The ASTM D-86 test suffers from several drawbacks, including large uncertainties in the temperature measurements and little theoretical significance.^{5,6}

In an effort to remedy these and other shortcomings, an improved distillation apparatus and measurement method was recently developed, the details of which have been described previously.^{5,7–10} Improvements to the traditional distillation apparatus included reduced uncertainty in the temperature and volume measurements (to 0.05 °C and 0.05 mL, respectively),

temperature control using a model-predictive temperature controller, and a composition-explicit data channel via a modified receiver adapter that allows for on-the-fly sampling of the distillate. This approach also provides important advantages over other methods, such as the simulated distillation method embodied in procedures such as ASTM D-2887. In that method, for example, one uses the gas chromatographic behavior of a suite of compounds as a frame of comparison with a fuel. The very significant advantage offered by the approach discussed in this paper is the ability to model the distillation curve resulting from our metrology with an equation of state. We have applied this advanced approach to the distillation curve to a variety of mixtures that include simple *n*-alkanes,⁵ gas turbine fuels,^{8,11} gasolines,¹² and rocket propellant.⁸

While the improvements made thus far have been of value, we recognize that the information content of the distillation curve can be extended much further. For instance, an additional composition measurement that would be of great interest for real fuels is the total sulfur content of the distillate at each volume fraction. Many sulfur impurities (such as H₂S, mercaptans, and elemental sulfur) can be corrosive, and therefore, their presence in fuels is undesirable. Additionally, knowledge of the temperature at which the sulfur impurities appear during the distillation of a fluid aids in the design of refinery processes.

* To whom correspondence should be addressed. Telephone: 303-497-5158. Fax: 303-497-5927. E-mail: bruno@boulder.nist.gov.

(1) Leffler, W. L. *Petroleum Refining in Nontechnical Language*; PennWell: Tulsa, OK, 2000.

(2) Kister, H. Z. *Distillation Operation*; McGraw-Hill: New York, 1988.

(3) Kister, H. Z. *Distillation Design*; McGraw-Hill: New York, 1991.

(4) Standard test method for distillation of petroleum products at atmospheric pressure, ASTM Standard D 86-04b. *Book of Standards*; American Society for Testing and Materials: West Conshohocken, PA, 2004; Vol. 05.01.

(5) Bruno, T. J. Improvements in the measurement of distillation curves: Part 1. A composition-explicit approach. *Ind. Eng. Chem. Res.* **2006**, *45* (12), 4371–4380.

(6) Eckert, A. B.; Vanek, T. Procedures for the selection of real components to characterize petroleum mixtures. *Chem. Pap.* **2003**, *57* (1), 53–62.

(7) Bruno, T. J. Method and apparatus for precision in-line sampling of distillate. *Sep. Sci. Technol.* **2006**, *41* (2), 309–314.

(8) Bruno, T. J.; Smith, B. L. Improvements in the measurement of distillation curves: Part 2. Application to aerospace/aviation fuels RP-1 and S-8. *Ind. Eng. Chem. Res.* **2006**, *45* (12), 4381–4388.

(9) Smith, B. L.; Bruno, T. J. Advanced distillation curve measurement with a model predictive temperature controller. *Int. J. Thermophys.* **2006**, *27* (5), 1419–1434.

(10) Bruno, T. J.; Smith, B. L. Enthalpy of combustion of fuels as a function of distillate cut: Application of an advanced distillation curve method. *Energy Fuels* **2006**, *20* (5), 2109–2116.

(11) Smith, B. L.; Bruno, T. J. Improvements in the measurement of distillation curves: Part 4. Application to the aviation turbine fuel jet-A. *Ind. Eng. Chem. Res.* **2007**, *46* (1), 310–320.

(12) Smith, B. L.; Bruno, T. J. Improvements in the measurement of distillation curves: Part 3. Application to gasoline and gasoline + methanol mixtures. *Ind. Eng. Chem. Res.* **2007**, *46* (1), 297–309.

This is especially clear in the case of fuels and lubricants. Hence, determining the total sulfur concentration at each volume fraction during the distillation of a fluid is of practical importance.

Corrosivity—The Copper Strip Corrosion Test (CSCT).

The corrosivity of certain sulfur species in fluid is usually determined by use of Standard Test Method D-1838 or D-130 (for liquefied petroleum gas and less volatile petroleum products, respectively), the CSCT.^{13,14} In these tests, a strip of cleaned, polished copper (12.5 mm wide, 1.5–3.0 mm thick, and 75 mm long)¹³ is placed in a vessel that has been rinsed with water and then filled with an appropriate quantity of fluid. The filled vessel is then maintained at a predetermined temperature, ranging from 38 °C (100 °F) to 100 °C (212 °F), for 1–3 h (the temperature and time being determined by the characteristics of the fluid under study).¹³ Then, the strip is removed from the fluid and immediately “read”.

Reading a copper strip is done by a comparison with lithographed standard strips provided by the ASTM. While it is not possible to reproduce the lithograph in this paper, we can describe it in general terms. The lithographs are divided into five classifications. First, a pristine, freshly polished strip is displayed on the ASTM lithograph; this pristine strip does not have a rating beyond “freshly polished”. Next, four levels of progressive sulfur-related corrosion are presented: level 1 (with 1a and 1b, slight tarnish), level 2 (with 2a–2e, moderate tarnish), level 3 (with 3a–3b, dark tarnish), and level 4 (with 4a–4c, severe corrosion). Strips 2c and 3b are both designated by ASTM as “multicolored”, while the remaining 10 standard strips have only one color descriptor.

Although the CSCT method is a well-established standard, it is both qualitative and subjective. Some disadvantages of the CSCT include (a) all persons see color differently, which can result in different readings of the same strip by different operators; (b) the readings can be lighting-dependent; (c) the lithograph has a nonlinear response progression (for example, 2d is vastly different from 2c; 2e is similar to 1a; and 3a is only slightly darker than 1b); (d) the strips must be read immediately after being removed from the fluid, which is sometimes difficult; (e) a freshly prepared strip never looks like that shown on the lithograph; (f) some of the color descriptors used on the lithograph, such as claret, are regionally uncommon and can be confusing; (g) the results of the test are very dependent upon strip preparation; and (h) failures can be caused by traces of some sulfur impurities and large amounts of others. Furthermore, the proper procedure for the CSCT is not always followed (including residence time, temperature, sampling, and proper use of the lithograph). Additionally, it has been noted that it is “...a rare occurrence to obtain a strip in routine work exactly matching any of these standards...”.¹⁵ Clearly, a more quantitative and objective interpretation of the results of a CSCT is desirable.¹⁶

In earlier work, we sought to make the interpretation of the CSCT results more quantitative and objective by analyzing strips with mathematical color spaces.¹⁷ Pinpointing a color in color space is analogous to locating a position on a map with coordinates.¹⁸ Three of the most common color spaces are RGB,

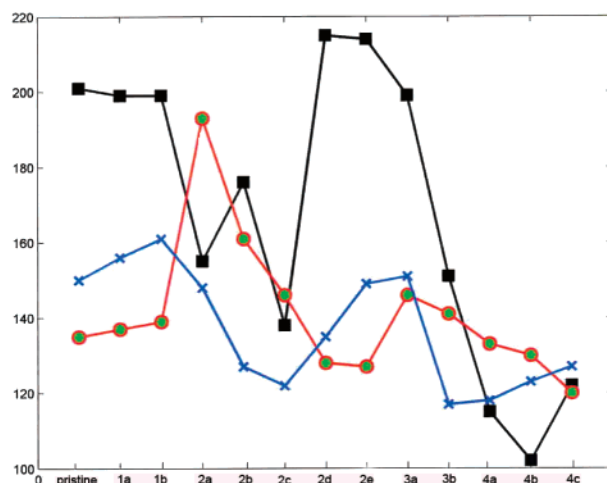


Figure 1. Measurement of the L* (black line with filled square markers), a* (red line with green-filled circle markers), and b* (blue line with cross markers) values for the ASTM-provided lithograph standard.

HSB, and L*a*b*. The RGB color space uses red, green, and blue axes; the HSB color space uses hue, saturation, and brightness axes, and the L*a*b* color space uses lightness (L*), the position on a continuum between red and green (a*), and the position on a continuum between yellow and blue (b*) for its axes. Of the common color spaces, the L*a*b* color space is the most complete, perceptually linear color model for describing all of the colors visible to the naked eye. Due to the advantages of the L*a*b* color space, we used the L* axis to quantitatively measure the corrosion of copper strips used for CSCTs as part of earlier work to improve the CSCT.¹⁷

As a further refinement of the CSCT, we explored the application of very small, circular copper coupons that fit in the bottom of autosampler vials in place of the standard oblong strips.¹⁹ There are several advantages to these small coupons. The reduced scale makes the test applicable to small samples, an important factor when the sample supply is limited or hazardous. The small (and inexpensive) coupons are amenable to archiving as a permanent record of each test. There is an overall reduction in chemical waste and potential for automated analysis when autosampler vials are used as reaction vessels. Moreover, the symmetric circular geometry facilitates the analysis of the images with L*a*b* color spaces described above, and the small size of the coupon can reduce staining (when the source of the stain is the presence of multiple phases in contact with the larger copper strips¹⁶).

Before applying color space analysis to the copper coupons, the L* values of each strip on the ASTM-provided lithograph were measured. A summary of the measurement is provided in Figure 1.¹⁷ Then, the L* values of copper strips used for CSCTs were measured and compared to the L* values measured for the lithograph. In this manner, the CSCT results can be quantitatively and objectively interpreted, avoiding many of the disadvantages of CSCT interpretation listed earlier.

(13) Standard test method for detection of copper corrosion from petroleum products by the copper strip tarnish test, ASTM Standard D 130. American Society for Testing and Methods: West Conshohocken, PA, 2004.

(14) Standard test method for detection of copper corrosion by liquefied petroleum (LP) gases, ASTM Standard D 1838-91. American Society for Testing and Materials: West Conshohocken, PA, 1991 (reapproved 2001); p 1.

(15) Matthews, F. W. H.; Parsons, D. F. The copper-strip test—A study of current methods of interpretation and an examination of proposed new procedures. Proceedings of the Mid-year Meeting, American Petroleum Institute: Washington, D.C., 1950; Vol. 30M, pp 24–37.

(16) Andersen, W. C.; Abdulgatov, A. I.; Bruno, T. J. The ASTM copper strip corrosion test: Application to propane with carbonyl sulfide and hydrogen sulfide. *Energy Fuels* **2003**, *17* (1), 120–126.

(17) Andersen, W. C.; Straty, G. C.; Bruno, T. J. Improving the copper strip corrosion test. Proceedings of the GTI Natural Gas Technologies Conference and Exhibition, Phoenix, AZ, 2004.

(18) Poynton, C. www.poynton.com/PDFs/ColorFAQ.pdf (accessed December 15, 2006).

(19) Ott, L. S.; Bruno, T. J. Modifications to the copper strip corrosion test for the measurement of sulfur-related corrosion. *J. Sulfur Chem.* **2007**, in press.

Total Sulfur Concentration. In the case of fluid corrosivity caused by sulfur impurities, we can apply a specific and quantitative approach to the analysis: gas chromatography with sulfur chemiluminescence detection (GC–SCD). GC–SCD is a rapid method that responds in an equimolar fashion to the total sulfur content. In an initial experiment, rocket propellant-1 was spiked with 1 ppm ethyl mercaptan and the 35% volume fraction was analyzed by GC–SCD.⁸ These results indicated that the advanced distillation curve method coupled with GC–SCD is an appropriate and rapid technique for quantitating the sulfur content at each desired volume fraction of the distillate. Furthermore, quantitating the total sulfur concentration responsible for the CSCT result at each volume fraction would be a valuable fuel design parameter.

Experimental Section

The *n*-hexane used as a solvent in this work was obtained from a commercial supplier and was analyzed by gas chromatography (30 m capillary column of 5% phenyl–95% dimethyl polysiloxane having a thickness of 1 μm and a temperature program from 50 to 170 $^{\circ}\text{C}$, with 5 $^{\circ}\text{C}$ per minute) using flame ionization detection and mass spectrometric detection. These analyses revealed the purity to be approximately 99.95%, and the fluid was used without further purification.

The *n*-decane (C_{10}) and *n*-tetradecane (C_{14}) used in this work were obtained from a commercial source. The fluids had a purity specification of 99.9% (mass/mass), which was verified by gas chromatography. The fluids were therefore used without further purification. Stock solutions of 50:50 (mol/mol) C_{10} : C_{14} were prepared volumetrically and stored sealed in 500 mL plastic bottles at 7 $^{\circ}\text{C}$.

H_2S was obtained from a commercial supplier with a purity specification of >99.5% (mass/mass). The stock solutions of C_{10} : C_{14} were bubbled with the H_2S for predetermined amounts of time to dissolve variable quantities of this corrosive sulfur compound. The dimethyl sulfoxide that was used for calibration of the sulfur chemiluminescence detector was obtained from a commercial source with a stated purity of 99.9% (mass/mass). The purity had been verified in earlier work by GC–SCD, and the fluid was used without further purification.

Advanced Distillation Curves. For each experiment, 200 mL of a C_{10} : C_{14} solution with dissolved H_2S was placed into the boiling flask of the distillation curve apparatus.^{5,9} The thermocouples were then inserted into the proper locations to monitor T_k , the temperature in the fluid, and T_b , the temperature at the bottom of the takeoff position in the distillation head. Enclosure heating was then commenced with a four-step program based on a previously measured distillation curve.⁵ Volume measurements were made in the level-stabilized receiver.

The distillation curves were measured at ambient atmospheric pressure. The pressure was measured with an electronic barometer; the expanded total uncertainty ($k = 2$) in the pressure measurements was 0.003 kPa. Distillation temperature readings were corrected for what should be obtained at standard atmospheric pressure. This was done with the modified Sidney Young equation, in which the constant term was assigned a value of 0.000 109.^{20–22} This value corresponds to a carbon chain of 12. The magnitude of the correction depends upon the extent of departure from standard atmospheric pressure. The location of the laboratory in which the measurements reported herein were performed is approximately 1650 m above sea level, resulting in a typical temperature correction of approximately 7 $^{\circ}\text{C}$.

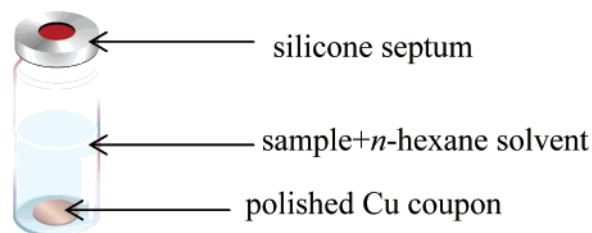


Figure 2. Drawing of an autosampler vial prepared with the *n*-hexane solvent and a polished Cu coupon for a CSCT.

To provide the composition channel to accompany the temperature information on the distillation curves, sample aliquots were withdrawn for 11 selected distillate volume fractions. To accomplish this, aliquots of $\sim 10 \mu\text{L}$ of emergent fluid were withdrawn from the sampling hammock in the receiver adapter with a blunt-tipped chromatographic syringe and added to a sealed autosampler vial containing a known mass of *n*-hexane solvent. A sample was withdrawn at the first drop of fluid from the condenser and then at each of 10 additional predetermined volume fractions of distillate, for 11 total sample aliquots. These withdrawn samples were then used for corrosivity measurements by the CSCT and chemical analysis by GC–SCD.

Corrosivity Measurements. The Cu coupons used for the CSCTs were punched from an electrolytic tough pitch copper sheet and were approximately 5 mm in diameter and 0.75 mm in thickness; these coupons fit conveniently in the bottom of wide-mouth GC autosampler vials. Each coupon had a slightly concave side and a flat side, resulting from punching the coupon out of the metal sheet. The coupons were polished on their flat sides with a rotary wheel coated with an abrasive polishing compound, similar to the ASTM recommendation of a “motor-driven machine using appropriate grades of dry paper or cloth”.¹³ The coupons were polished for 30–60 s, until the oxide layer atop each coupon was removed and the surface appeared uniformly smooth. The standards recommend a “final polishing” step with a larger mesh grit paper to roughen the surface of the copper; however, this step is impractical when using these small coupons. Moreover, the surfaces of the coupons are adequately rough because their surfaces have been polished only with a fine grit polishing compound, leaving some inherent roughness of the copper metal surface. Because only one side of each coupon was polished, the small coupons have only $1/220$ to $1/240$ of the surface area of the standard oblong strips (the precise ratio depending upon the thickness of the strip). The ASTM guidelines also recommend cleaning all metal dust and shavings from the copper surface with absorbent cotton before use.¹³ Consequently, the coupons were scrubbed with cotton swabs soaked in 50:50 acetone/toluene to remove any residual polishing compound. The polished coupons were stored in 50:50 acetone/toluene until use.

The autosampler vials used for CSCT vessels were first rinsed with approximately 1.5 mL of deionized water. This left a small amount of water in the vial, as specified in the standards.¹⁴ A Cu coupon was then removed from the acetone/toluene storage solution, rinsed in neat acetone, dried (to remove the residual solvent), and placed in the bottom of the vial. The vial was filled with ~ 0.7 mL of *n*-hexane and sealed with a crimp cap with a silicone septum (see Figure 2 for a drawing of a “prepared” vial). At each measured volume fraction, the distillate was injected into a prepared vial using the same chromatographic syringe with which the distillate was withdrawn from the sampling hammock.

After injection of the distillate into the vial, each vial was agitated on a vortex plate for 5 s to ensure sufficient mixing of the distillate. Then, each vial was further capped with a rubber cover over the crimp cap to minimize H_2S permeation and loss through the pierced septum. The rubber covers were fabricated by cutting the bottom off 1 mL rubber bulbs. Next, the vial was placed in a stirred water bath maintained at 38.5 $^{\circ}\text{C}$ (100 $^{\circ}\text{F}$) for 1 h as specified in the ASTM standards.^{13,14} After 1 h, the vial was removed from the water bath, its rubber cover was removed, the crimp cap was

(20) Young, S. Correction of boiling points of liquids from observed to normal pressures. *Proc. Chem. Soc., London* **1902**, 81, 777.

(21) Young, S. *Fractional Distillation*; Macmillan and Co., Ltd.: London, U.K., 1903.

(22) Young, S. *Distillation Principles and Processes*; Macmillan and Co., Ltd.: London, U.K., 1922.

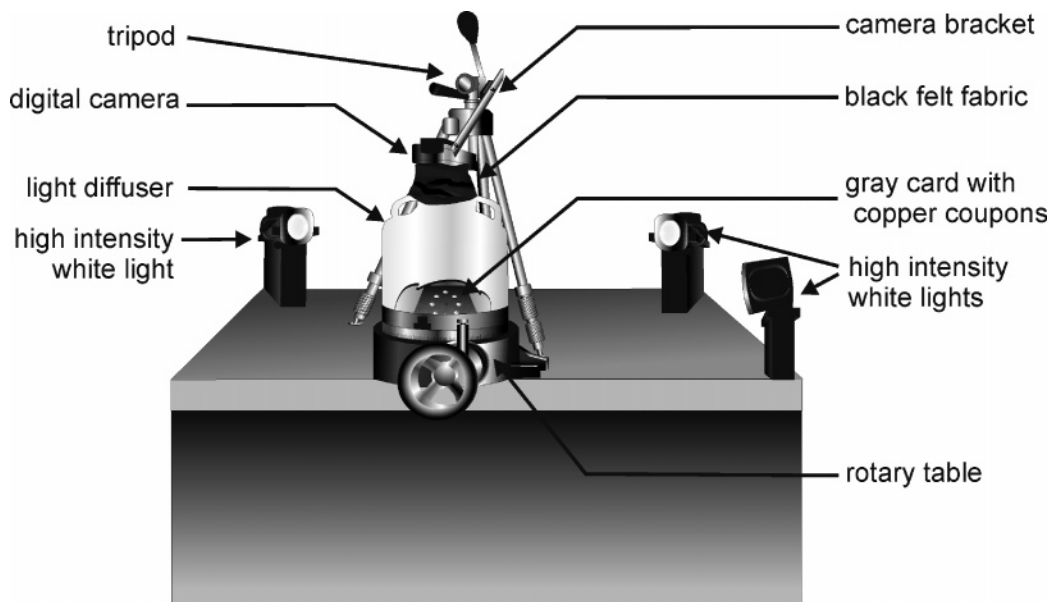


Figure 3. Schematic diagram of the setup used for digital imaging of the Cu coupons. Note that the gray card with the mounted copper coupons is underneath the light diffuser.

uncrimped, and the solution was decanted. The Cu coupons were then dried and rated using the ASTM D130/IP 154 lithograph.

Lightness Measurements. Since we desired a faithful digital reproduction of the Cu coupons, we performed a series of survey tests to determine how best to reproduce the visual appearance and features of the small coupons. These tests included making images of the coupons with several scanners and digital cameras. We found that the digital camera performed best and that the flat side of the coupon consistently provided the best image in terms of reproducing what is seen visually. Below, we describe the apparatus that we used to collect digital images; other apparatuses, such as commercial light sheds, might also be suitable.

For imaging the Cu coupons, photographer's gray cards were used to provide a background with a neutral reflectance of 18% (on the basis of the standard reflectance with which light meters are calibrated).²³ The Cu coupons from each CSCT were mounted with craft glue onto a gray card in a circular pattern. The circular pattern was used to promote uniform lighting conditions over the 11 coupons. Next, the gray card was centered on a rotary table typical of the type used in machine shop operations. A semi-opaque white light diffuser (made from a large polyethylene carboy) was used to cover the gray card on the rotary table. The diffuser was used to provide indirect lighting without reflection off the surfaces of the coupons. The digital camera was mounted on a tripod, suspending the camera directly atop the opening to the carboy. The mouth of the carboy was encircled with black felt to shield the camera from stray light. The room lights were extinguished, and the diffuser was illuminated with three high-intensity white lights (see Figure 3).

The camera was operated to collect image data in raw format; these images were subsequently converted to tif format. Next, the tif images were imported into a commercially available digital imaging software package, where the image was viewed in the $L^*a^*b^*$ color space. The software was used to capture the largest circular area of each coupon without including any coupon edges. The same size circular "lasso" was used for each coupon in a series, and these were viewed and analyzed in the $L^*a^*b^*$ color space.

To minimize uncertainty and avoid aberrant L^* measurements because of shadowing on the coupons, five images of each gray card (containing the coupons) were captured, rotating the circle of coupons about the center after each image was captured. The L^* values, which are reported herein, are a numerical average of the

five individual L^* images collected following the procedure outlined above. The standard deviation and standard uncertainty were calculated for each coupon.²⁴ The expanded ($k = 2$) uncertainty was between 5 and 6% of the mean value in each case.

As mentioned earlier, on a very small number of images, a shadow was cast on a coupon by (1) a slightly bent coupon, (2) uneven mounting of the coupon on the gray card, or (3) nonuniform lighting conditions. The presence of a shadow (not to be mistaken for corrosion) was detected by comparing the apparently shadowed coupon over the five digital images of the gray card; if the darkened area of the coupon appeared on different sides of the coupon or was not present in one or more of the images, it was determined to be a shadow. In the case of a shadow, the L^* value was measured by using an area of the coupon that did not include the shadowed (and thus an artificially low L^* valued) portion of the coupon. This area is necessarily smaller than the area described above, which was intended to capture the largest possible portion of the coupon. We found that this procedure did not markedly increase the uncertainty. Moreover, it was necessary to do this in only a few cases.

Additionally, a few coupons showed small, distinct, stained spots. The occurrence of stains on copper strips during the CSCT is well-known and discussed in the ASTM standards.^{13,14} In the case of stains, the L^* value of the coupon was determined by excluding the stained portion(s) in a similar manner to that described above for the shadowed coupons. This is consistent with the usual interpretation of CSCT strips as specified in the ASTM standards.

GC-SCD. The total sulfur content of each distillate fraction dissolved in *n*-hexane was analyzed on a commercially available gas chromatograph equipped with a sulfur chemiluminescence detector.²⁵ A background correction was performed using *n*-hexane; the nonzero response of the sulfur chemiluminescence detector to *n*-hexane was subtracted from each of the sample values to obtain the corrected sulfur signal. The total sulfur concentration in each vial was calculated by use of a calibration curve prepared with solutions of dimethyl sulfoxide. Additionally, a sample of each prepared stock solution of C_{10} - C_{14} with dissolved H_2S was analyzed by GC-SCD to determine the initial concentration of H_2S in each.

(24) Taylor, B. N.; Kayatt, C. E. *Guidelines for Evaluating and Expressing the Uncertainty of NIST Measurement Results*. NIST Technical Note 1297; National Institute of Standards and Technology: Gaithersburg, MD, 1994.

(25) Ryerson, T. B.; Dunham, A. J.; Barkley, R. M.; Sievers, R. E. Sulfur-selective detector for liquid-chromatography based on sulfur monoxide-ozone chemiluminescence. *Anal. Chem.* **1994**, *66* (18), 2841-2851.

(23) <http://www.acecam.com/magazine/gray-card.html> (accessed January 9, 2007).

Table 1. Complete Table of Distillation Temperatures, CSCT Ratings, Lightness Values, and Sulfur Concentrations for a Lower Initial Sulfur Concentration (3.8 mM) Sample

sample	volume fraction (%)	T_k (°C) ^a	CSCT	L*	[sulfur] (mM) ^b
A	0.025	199.0	3b	170	0.34
B	10	202.7	3b	96	0.28
C	20	208.0	3a	170	0.18
D	30	216.1	1a	198	
E	35	221.2	1a	200	
F	40	228.4	1a	199	
G	45	236.1	1a	199	
H	50	244.0	1a	202	
I	60	251.0	1a	201	
J	70	252.8	1a	201	
K	80	253.3	1a	201	

^a The kettle temperatures (T_k) have been corrected to 1 atm by the modified Sidney Young equation, as described earlier.⁵ The atmospheric pressure during this measurement was 83.5 kPa. ^b These sulfur concentrations were measured after the distillate was diluted in the *n*-hexane solvent, as detailed in the text.

Two approaches were tested to determine the best method for (simultaneously) measuring the total sulfur content by GC–SCD and performing a CSCT at each volume fraction of the distillation. In the first method, the sulfur analysis and the CSCT were carried out in two separate vials to avoid the reaction between H₂S and the Cu coupon during GC–SCD analysis; in the second method, the sulfur analysis and the CSCT were carried out in the same vial to measure the sulfur concentration and corrosivity of the same solution. We elected to use the second method to directly correlate the sulfur concentration and corrosivity. Consequently, we could determine quantitatively the concentration of H₂S required for each CSCT rating. Accordingly, each sample was analyzed by GC–SCD with the Cu coupon present in the bottom of the vial. Immediately after GC–SCD analysis, the vial was removed from the autosampler tray and placed in a water bath for a CSCT. Any reaction of H₂S with the Cu coupon during GC–SCD analysis would mean that the sulfur concentrations would be somewhat lower than the sulfur concentration immediately after injection of the distillate. Polishing only the flat side of the coupons reduced the reaction of H₂S with the coupon during GC–SCD analysis because the rounded side retained a passivating oxide layer.

In the course of method development, we observed that H₂S could be lost through the septa of the autosampler vials. This loss was evidenced by a continuously decreasing sulfur signal over the course of five replicate sample injections and no detectable sulfur signal above the background signal of the solvent approximately 2 h after the first sampling. It was thus important to develop the sulfur analysis protocol with particular attention to this loss. Two approaches were used to determine the sulfur content in each fraction. First, the sulfur concentration was measured using only one (immediate) injection, when, presumably, little or no H₂S had been lost through the septum. Second, five replicate injections were plotted against a time axis (the time required for the injections), and the sulfur concentration at time zero was obtained by extrapolation. These two results yielded initial sulfur concentrations that were within 10% of each other. The former method was selected on the basis of its speed, which was essential given our choice of using one vial for both GC–SCD and CSCT analysis.

Results and Discussion

Experiments with two separate fluid mixtures of *n*-decane plus *n*-tetradecane are detailed below. These fluids had initial H₂S concentrations that differed approximately 15-fold. Eight additional distillations with initial H₂S concentrations that varied from 3 to 60 mM were performed with this new metrology but are not reported in detail herein.

Distillation Curve with a Lower Initial Sulfur Concentration. Table 1 shows the complete results for the distillation

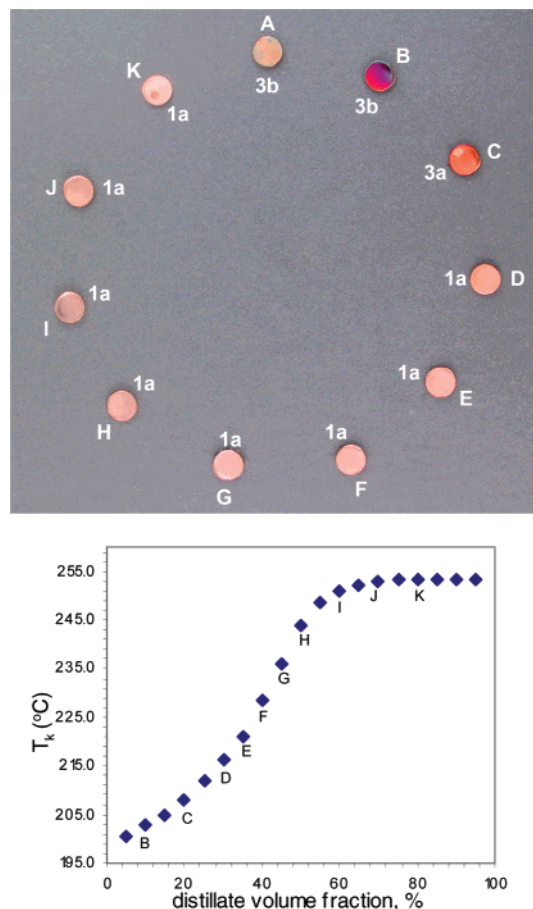


Figure 4. Copper coupons from a low initial sulfur concentration experiment with sample labels and CSCT ratings (top) and a typical distillation curve for the H₂S-spiked C₁₀:C₁₄ mixture (bottom). The sample labels on the distillation curve indicate where the distillate cuts were removed for GC–SCD and copper strip corrosion testing.

temperatures, CSCT ratings, L* values, and total sulfur concentration for a sample of 50:50 mol % C₁₀:C₁₄ with an initial H₂S concentration of 3.8 mM. Additionally, Figure 4 shows the 11 Cu coupons mounted on a gray card and the distillation curve for the fluid with fractions B–K noted on the curve (fraction A is the first drop down the condenser, with a volume fraction of approximately 0.025%).

The third column of Table 1 reports T_k , corrected to standard atmospheric pressure with the Sidney Young equation, at each of 11 volume fractions measured during distillation of the fluid. The T_k values reported in Table 1 are within 0.6% of our earlier report of distillation of C₁₀:C₁₄ without dissolved H₂S.⁵ Additionally, the temperature measured in the distillation head (T_h) reproduces the same behavior as C₁₀:C₁₄ without dissolved H₂S. T_k leads T_h by an average of 20 °C until the end of the distillation, when the two temperatures are within 1 °C (with T_k still leading T_h). Therefore, the addition of 3.8 mM H₂S does not appear to affect the overall distillation curve of 50:50 mol % C₁₀:C₁₄.

The results of the CSCT in the fourth column of Table 1 show dark tarnishing for the first three coupons, corresponding to 0.025, 10, and 20% of the distillate volume (and distillation temperatures of 199.0, 202.7, and 208.0 °C, respectively). Coupons A and B were both rated 3b, while coupon C was rated 3a. One advantage to capturing digital images of the Cu coupons is the ability to magnify the images on the a computer screen and rate them using the very large images, as we did for all of the images shown herein. The remaining coupons (for

Table 2. Complete Table of Distillation Temperatures, CSCT Ratings, Lightness Values, and Sulfur Concentrations for a Higher Initial Sulfur Concentration (57 mM) Sample

sample	volume fraction (%)	T_k (°C) ^a	CSCT	L*	[sulfur] (mM) ^b
A	0.025	199.3	4a	78	6.40
B	10	202.3	3b	105	3.00
C	20	207.6	3b	158	1.44
D	30	215.2	3a/3b	170	0.73
E	35	220.0	3a/3b	142	0.54
F	40	226.6	2b	109	0.37
G	45	233.8	2b	134	0.38
H	50	241.6	2e	184	0.16
I	60	250.1	1a/1b	199	
J	70	252.7	1a/1b	201	
K	80	253.4	1a/1b	193	

^a The distillation temperatures have been corrected to 1 atm by the modified Sidney Young equation, as described earlier.⁵ The atmospheric pressure during this measurement was 82.4 kPa. ^b These sulfur concentrations were measured after diluting the distillate in the *n*-hexane solvent, as detailed further in the text.

fractions D–K) were all rated 1a, corresponding to slightly tarnished coupons.¹³ The 1a rating is typically a passing rating for fuels and lubricants and is an indication of low corrosivity toward copper.

The fifth column of Table 1 contains the L* values for each CSCT coupon. The L* values for coupons A and B, both of which have a CSCT rating of 3b, are significantly different from one another because each coupon matched a separate region of the “multicolored”¹³ lithograph standard strip. This is not a disadvantage of the CSCT or the L*^a*b* analysis; it is simply an inherent characteristic of the approach. Coupon C has a L* value of 170, which is comparable with, although somewhat lower than, the L* value shown for strip 3a in Figure 1. The 3a strip on the lithograph is not uniform; the variations in the “magenta overcast”¹³ is likely the reason for the difference in the measured L* values for the lithograph and coupon C. The coupons that received ratings of 1a (coupons D–K) had measured L* values in the range of 195–200, which correlates very well with the L* values measured for the lithograph standard (recall Figure 1).¹⁷

Finally, the sixth column of Table 1 contains the total sulfur content of each distillate cut dissolved in the *n*-hexane solvent as measured by GC–SCD. Only the sulfur content for the first three fractions are reported because the sulfur content for the remaining fractions was so low that it could not be quantified above the background signal of the *n*-hexane solvent. An important result is that only the coupons that showed corrosion by the CSCT had a sulfur content measurable by GC–SCD. Clearly, the CSCT is a valid and valuable approach when used properly. The total sulfur content for the diluted distillate ranged from 0.34 to 0.18 mM for the first three distillate cuts (samples A–C).

Of note here is that the sulfur concentrations shown in the final column of Table 1 were measured for the distillate diluted in the *n*-hexane solvent. It is these concentrations of sulfur that are responsible for the CSCT results and L* values shown in Table 1. The concentration of H₂S in the undiluted distillate can be calculated from the known masses of *n*-hexane and distillate in each sample vial. For volume fractions A, B, and C, the undiluted concentrations of H₂S are 27, 28, and 16 mM, respectively. These distillate fractions have sulfur concentrations higher than that of the stock solution because all detectable H₂S contained in the 200 mL starting solution is concentrated in and emerges with the first 20% (40 mL) of the distillate.

Distillation Curve with a Higher Initial Sulfur Concentration. Table 2 shows the complete results for the distillation temperature, CSCT ratings, L* values, and total sulfur concen-

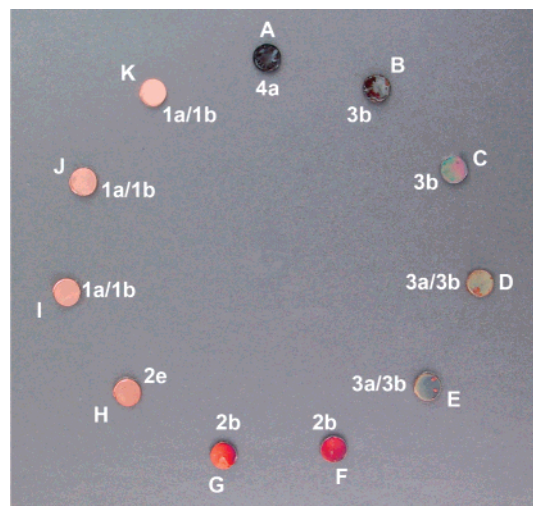


Figure 5. Copper coupons from a higher initial sulfur concentration (57 mM) distillation.

tration for a sample of C₁₀:C₁₄ with a higher, 57 mM initial concentration of H₂S (~15-fold higher initial concentration than the previous experiment). Additionally, Figure 5 shows the 11 Cu coupons from this distillation mounted on a gray card.

The distillation temperatures, T_k , shown in the third column of Table 2 are within 1% of the distillation temperatures reported in Table 1. Additionally, the behavior of T_h is consistent with the experiment reported in Table 1 and our earlier distillations of C₁₀:C₁₄ without dissolved H₂S.⁵ These results show that, even with this ~15-fold higher initial concentration of H₂S, the presence of H₂S does not significantly change the distillation curve of 50:50 mol % C₁₀:C₁₄.

The results of the CSCT presented in the fourth column of Table 2 show tarnishing for the first eight coupons (corresponding to a distillation temperature of 241.6 °C for the eighth coupon). In this sample with a 15-fold higher initial sulfur concentration, the fluid was corrosive for 50% of the distillate, compared to 20% in the lower concentration experiment. Because the two distillations were carried out with the same temperature program on the model-predictive temperature controller, the mass flow rate of the distillate through the apparatus is the same (within the sensitivity of the measurement) and the presence of H₂S in eight fractions is not simply an artifact of the distillation rate. Indeed, a separate distillation with an initial H₂S concentration of 60 mM with the temperature controller programmed such that the distillation took twice the amount of time also showed that the fluid was corrosive for the first 50% of the distillate. Therefore, the presence of H₂S in the distillate does not depend upon the distillation rate, and the 15-fold higher concentration of H₂S results in the presence of detectable H₂S through a greater volume fraction of the distillate.

The fifth column of Table 2 shows the L* values measured for each coupon. Coupon A, the most corroded of all 11 coupons, has the lowest measured L* value of 79. Coupon H, which has a 2e rating, has a rather high L* value of 184; however, this value is consistent with the measured L* value for the lithograph standard (again, recall Figure 1).¹⁷ Coupons I–K, with ratings of 1a/1b on the CSCT, show very high L* values around 200. Coupons B–G were all given the “multicolored” 2c or 3b rating. As such, they match (or are compatible with) varying parts of the 2c or 3b lithograph images. Overall, the L* values measured for the coupons shown in Figure 5 are consistent with both the L* values measured for the coupons shown in Figure 4 and the lithograph standard shown in Figure 1.

The sixth column of Table 2 shows the total sulfur content of each distillate cut dissolved in the *n*-hexane solvent as measured by GC-SCD. As in the lower initial sulfur concentration experiment, only the coupons that showed corrosion above a CSCT rating of 1 had measurable sulfur concentrations by GC-SCD. Additionally, higher concentrations of sulfur correlate well with more extensive corrosion of the Cu coupons as measured by the CSCT. In agreement with the results shown in Table 1, the coupons that rate above 1a or 1b on the CSCT have a total H₂S concentration of ≥ 0.16 mM (8 ppm). This concentration is consistent with our previous study, which found that H₂S concentrations up to 6 ppm will receive a 1a rating in liquefied petroleum gas.¹⁶ Both 6 and 8 ppm of H₂S are significantly higher than the 0.35–1 ppm of H₂S that engineering literature suggests would cause a CSCT rating higher than 1.¹⁶

The concentration of sulfur in the emergent, undiluted distillate fractions was again calculated. These sulfur concentrations ranged from the highest concentration of 1.6 M for fraction A to the lowest concentration of 12 mM for sample H. Again, these distillate fractions were found to have higher sulfur concentrations than that of the stock solution due to H₂S being concentrated in the first 50% (100 mL) of the fluid.

Conclusions

The work reported herein demonstrates further development of the advanced distillation curve method, extending the method

to the analysis of corrosive fluids. With these measurements, four channels of data are collected at each predetermined volume fraction: distillation temperatures (thermodynamic state point and historical), CSCT rating, L* value, and total sulfur concentration. A comparison of the distillation curves reported herein with our earlier work⁵ reveals that initial concentrations of up to 57 mM H₂S do not affect the distillation curve of 50:50 mol % C₁₀:C₁₄. The subjective CSCT ratings were augmented by objective, measured L* values for each Cu coupon. Additionally, the L* values for the Cu coupons also reproduced the L* values of the lithograph standard, with the known exception of the standard strips that are described as “multi-colored”.¹⁹ Finally, a total sulfur analysis on each distillate cut allows for (1) the quantitation of the H₂S concentration responsible for each CSCT rating (and its corresponding L* value) and (2) the calculation of the emergent fluid H₂S concentration at each measured volume fraction. These data channels applied to the advanced distillation curve metrology are especially applicable to real fuel feedstocks, in which the presence of corrosive acidic species is common.

Acknowledgment. This work was performed while L.S.O. held a National Academy of Science/National Research Council Postdoctoral Associateship Award at NIST.

EF070195X